Available online at www.sciencedirect.com

SCIENCE DIRECT®

Journal of Non-Crystalline Solids 345&346 (2004) 88–92

JOURNAL OF NON-CRYSTALLINE SOLIDS

www.elsevier.com/locate/jnoncrysol

Section 1: Glass Structure

Structural and optical characterization of amorphous $As_{40}S_{60}$ and $As_{40}Se_{60}$ films prepared by plasma-enhanced chemical vapor deposition

J.M. González-Leal [a,*], R. Prieto-Alcón [b], M. Vlcek [c], E. Márquez [b]

[a] *Department of Chemistry, University of Cambridge, Lensfield Road, CB2 1EW Cambridge, UK*
[b] *Departamento de Física de la Materia Condensada, Facultad de Ciencias, Universidad de Cádiz, 11540 – Puerto Real (Cádiz), Spain*
[c] *Department of General and Inorganic Chemistry, University of Pardubice, 53210 – Pardubice, Czech Republic*

Abstract

Amorphous chalcogenide films of chemical compositions $As_{40}S_{60}$ and $As_{40}Se_{60}$ have been prepared by plasma-enhanced chemical vapor deposition. An improved optical characterization method suitable for non-uniform thin films, which also takes into consideration the weak absorption in the substrate, has successfully been applied. The values of the average thickness and thickness variation, $\bar{d}$ and Δd, respectively, were crossed-checked with those measured by use of a surface-profiling stylus instrument, and differences between the directly measured and the optically calculated values were, in all cases, less than 2%. A comparison between the structural and optical properties of these PECVD films, and those of the same chemical composition prepared by thermal evaporation, is systematically made in this paper.

IDT: A200; C140; C185; F135; O110
PACS: 78.20.−e; 78.66.Jg; 78.20.Ci; 78.40.Fy

---

1. Introduction

The preparation conditions of amorphous thin films affect significantly their properties [1,2]. This implies the need to control the parameters that are related to the particular deposition technique being used. Thus, to synthesize films by plasma-enhanced chemical vapor deposition (PECVD), the precursor gas ratio, for instance, plays a crucial role in the final composition of the deposited material, while in the case of films prepared by thermal evaporation (TE) the deposition rate is a key factor.

In the present work we have deposited amorphous $As_{40}S_{60}$ (As_2S_3) and $As_{40}Se_{60}$ (As_2Se_3) thin films onto glass substrates by both techniques, and have calculated their optical properties by means of a characterization method that does not neglect the weak absorption in the substrate [3]. X-ray diffraction measurements, along with FTIR and Raman spectroscopies, have been used to complete the structural study of our samples, and a comparison between the PECVD and thermally evaporated films with the same chemical composition has been made.

2. Experimental details

Amorphous $As_{40}S_{60}$ and $As_{40}Se_{60}$ thin films have been deposited in a plasma-discharge stainless steel reactor by use of an rf discharge (13.56 MHz) between two

---

[*] Corresponding author. Tel.: +44 1223 3 36532; fax: +44 1223 3 36362.
E-mail addresses: jmg62@cam.ac.uk (J.M. González-Leal), juanmaria.gonzalez@uca.es (J.M. González-Leal).

0022-3093/$ - see front matter © 2004 Published by Elsevier B.V.
doi:10.1016/j.jnoncrysol.2004.08.001

parallel plate electrodes, 8 cm in diameter. The distance between those electrodes was 3 cm for all the experiments carried out. Electronic mass flow controllers were used in order to control gas flows. The total gas pressure was measured and automatically regulated through a butterfly valve by a Baratron pressure gauge. Glass substrates were carefully cleaned and fixed on both electrodes. Depositions were made without additional heating of the substrate, but due to heating by the plasma, the temperature may rise upto approximately 50 °C. The precursor gases were high-purity hydrides, H_2S, H_2Se and AsH_3, pure or diluted in hydrogen (15 vol.% of the hydrides), and introduced in the reaction chamber setting the gas flow at 10 sccm. Several depositions were carried out using different pressures in the chamber, as well as different AsH_3/H_2S and AsH_3/H_2Se gas ratios - the pressures were in the range 0.025–1 mbar and the gas ratios in the interval between 1/0 and 1/99. Amorphous $As_{40}S_{60}$ films were obtained at 0.20 mbar, $AsH_3/H_2S = 1/19$, and an rf power of 15 W, while for the amorphous $As_{40}Se_{60}$ films the preparation conditions were 0.25 mbar, $AsH_3/H_2S = 2/1$ and an rf power of 60 W.

The chemical compositions of the films were determined by EDAX and differences between real and nominal compositions were always less than 10%. The amorphous nature of the films was checked by means of X-ray diffraction measurements. All the samples were stored in complete darkness and in a moisture-free environment to prevent them from hydrolysis and possible oxidation.

The optical transmission spectra at normal incidence were obtained over the 400–2500 nm spectral range by a double-beam UV/Vis/NIR spectrophotometer (Perkin-Elmer, model Lambda-19). The area of illumination over which a single transmission spectrum was obtained is 1 mm × 10 mm.

3. Results

Fig. 1 shows the optical transmission spectra corresponding to representative samples of chemical compositions $As_{40}S_{60}$ and $As_{40}Se_{60}$, deposited by PECVD and TE. Both PECVD and TE films show wedge-shaped profiles clearly evidenced by their corresponding *shrunk* transmission spectra [4]. Nevertheless, this feature is more significant in the PECVD samples than in the TE ones. Hence, it was necessary to take into account this particular geometry when determining their optical constants. An enhanced version [3] of the envelope method first developed by Swanepoel [4,5], which considers the absorption in the glass substrate, was used to characterize optically and geometrically our non-uniform samples. This method enabled the determination of the average film thickness, $\bar{d}$, and refractive index, n, of the chalcogenide films with an accuracy better than 1%, as well as a parameter modelling the non-uniformity in thickness, Δd, with an accuracy better than 2%. The values of the average thickness and thickness variation, $\bar{d}$ and Δd, respectively, were crossed-checked with those measured by use of a surface-profiling stylus instrument, and differences between the directly measured and the optically calculated values were, in all cases, less than 2%. Values obtained for $\bar{d}$ and the wedging parameter, Δd, for the films whose transmission spectra are shown in Fig. 1, are listed in Table 1.

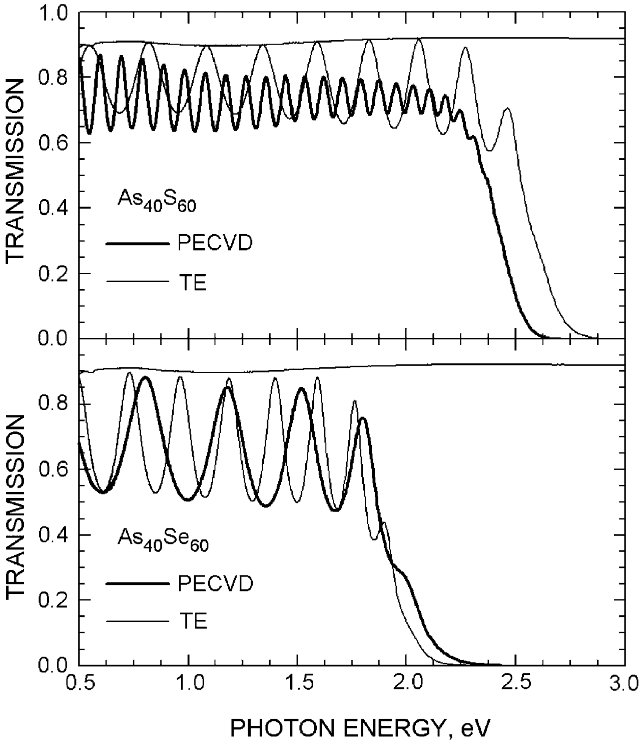

Fig. 1. Transmission spectra at normal incidence corresponding to films of chemical compositions $As_{40}S_{60}$ and $As_{40}Se_{60}$, prepared by PECVD and TE.

The set of values of the refractive index obtained from the application of the above-mentioned interference method, at those wavelengths where the transmission spectra and their two envelopes are *tangential* [3], were analyzed on the basis of the Wemple-DiDomenico (WDD) dispersion model [6], which is based on the single-oscillator approach:

$$n^2(\hbar\omega) = 1 + \frac{E_o E_d}{E_o^2 - (\hbar\omega)^2}, \qquad (1)$$

where $\hbar$ is Planck's constant divided by 2π, $\hbar\omega$ is the photon energy, E_o is the single-oscillator energy and E_d is the dispersion energy. Plotting $(n^2-1)^{-1}$ against $(\hbar\omega)^2$ allows one to determine the oscillator parameters by fitting a straight line to the experimental points, as shown in Fig. 2. Then, E_o and E_d are determined directly from the slope, $(E_o E_d)^{-1}$, and the intercept on the

Table 1
Values of the average film thickness, $\bar{d}$, wedging parameter, Δd, WDD optical dispersion parameters, E_o and E_d, the effective As coordination number, N_c, inferred from the E_d values, the refractive index for $\hbar\omega \to 0$, $n(0)$, and the Tauc gap, E_g^{opt}, and slope, $B^{1/2}$, for $As_{40}S_{60}$ and $As_{40}Se_{60}$ films prepared by PECVD, and for films of the same composition prepared by TE. Values of the dispersion parameters, found in the literature, for films of the same compositions prepared by TE, are also presented for comparison

Technique-composition	$\bar{d}$ (nm)	Δd (nm)	E_o (eV)	E_d (eV)	N_c	$n(0)$	E_g^{opt} (eV)	$B^{1/2}$ ($cm^{-1/2}$ $eV^{-1/2}$)	References
PECVD-$As_{40}S_{60}$	2646 ± 13	50 ± 2	4.90 ± 0.02	21.99 ± 0.07	3.2 ± 0.3	2.343 ± 0.001	2.37 ± 0.01	790 ± 2	
TE-$As_{40}S_{60}$	1098 ± 4	9 ± 1	5.11 ± 0.01	20.65 ± 0.04	3.0 ± 0.3	2.245 ± 0.001	2.43 ± 0.01	900 ± 2	
			4.80	22.14					[8]
			4.85	23.00					[9]
			4.75	22.70					[10]
			4.70	22.80					[11]
			4.55	21.50					[12]
			4.80	23.99					[13]
			4.65	18.51					[14]
PECVD-$As_{40}Se_{60}$	563 ± 3	20 ± 1	3.70 ± 0.06	22.87 ± 0.40	3.3 ± 0.3	2.679 ± 0.004	1.77 ± 0.01	802 ± 1	
TE-$As_{40}Se_{60}$	911 ± 4	10 ± 1	3.74 ± 0.02	23.34 ± 0.14	3.4 ± 0.3	2.690 ± 0.002	1.79 ± 0.01	835 ± 1	
			3.77	23.31					[11]
			3.67	21.91					[15]

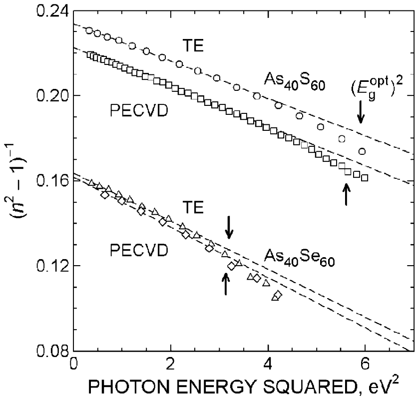

Fig. 2. Plot of the refractive-index factor $(n^2-1)^{-1}$ versus $(\hbar\omega)^2$, for $As_{40}S_{60}$ and $As_{40}Se_{60}$ films prepared by PECVD and also for films of the same chemical composition but prepared by TE. The arrows show the values of the optical bandgap squared, $(E_g^{opt})^2$, at which the experimental data depart from the linear behaviour. The optical bandgap is formally defined in the text, when analyzing the optical absorption spectra.

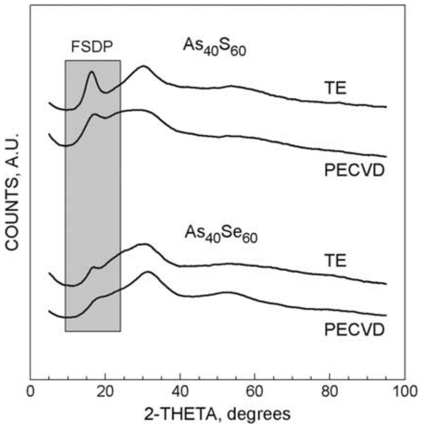

Fig. 3. X-ray diffraction patterns corresponding to $As_{40}S_{60}$ and $As_{40}Se_{60}$ films prepared by PECVD as well as those for films of the same chemical composition that have been prepared by TE.

vertical axis, E_o/E_d. Table 1 lists the values of the dispersion parameters for the PECVD films of compositions $As_{40}S_{60}$ and $As_{40}Se_{60}$, along with those corresponding to films of the same composition, but prepared instead by TE. Furthermore, in the same table are also shown the values for the static refractive index, $n(0)$, which have been obtained by extrapolation of Eq. (1) towards $\hbar\omega = 0$.

X-ray diffraction measurements were carried out in order to obtain structural information of the films. Fig. 3 shows the X-ray diffraction patterns of a-$As_{40}S_{60}$ and a-$As_{40}Se_{60}$ alloys prepared by PECVD, and also by TE. Note the presence of the first sharp diffraction peak (FSDP) in those diffraction patterns at $2\theta = 16.02°$ and $17.20°$, respectively, for S-based alloys, and $17.04°$ and $18.02°$ for the Se-based ones (all of them, at values of the modulus of the scattering vector, $Q \approx 1.1\,\text{Å}^{-1}$). This characteristic feature in the X-ray diffraction results on amorphous chalcogenides has been traditionally associated with the existence of medium-range structural order in non-crystalline solids [1]. Among the different models suggested stands out the one proposed by Elliott [7]. According to this model, the FSDP is due to the presence of an *ordered* pattern of interstitial voids in the amorphous matrix. In our particular case, this model would be interpreted with the presence of such a free volume surrounding the pyramidal units AsS_3 or $AsSe_3$.

4. Discussion

Values of the dispersion parameters E_o and E_d calculated for our PECVD and TE samples, along with those values reported by other authors for TE As_2S_3 and

As_2Se_3 films, are all listed in Table 1. It is observed that, in most cases, and especially in the case of the a-$As_{40}S_{60}$ alloy, the values presented by these authors are certainly quite different from those determined in the present work, for our TE films. Besides subtle compositional differences between those samples and ours, as well as, quite likely, differences in the preparation conditions, these discrepancies could be explained taking into account that, generally, in the cited references, application of the single-oscillator model is extended towards values of the refractive index beyond the transparency region, where this model is no longer valid. It should be noted that the calculation of E_o and E_d for a representative *a*-$As_{40}S_{60}$ film prepared by TE, considering in the WDD fit every single value of the refractive index up to a square photon energy, $(\hbar\omega)^2 \approx 6\,eV^2$, gave values of $4.90 \pm 0.02\,eV$ and $20.72 \pm 0.02\,eV$, respectively. Suffice to say that the agreement between these values and those presented in the literature is much better, although, as we mentioned before, it arises from an incorrect application of the single oscillator formula.

Returning the discussion to our particular results, it is observed that the E_o values of the PECVD films are slightly lower, for both As–S and As–Se systems, compared with those corresponding to the samples deposited by TE. This could be related to the fact that in the latter film-preparation technique, the formation of molecular species containing homopolar bonds of the type As–As, S–S and Se–Se, with higher bonding energies (382.0, 425.3 and 332.6 kJ/mol, respectively) than the heteropolar ones As–S and As–Se (379.5 and 96 kJ/mol, respectively) [16], would be favored.

On the other hand, the dispersion energy, E_d, obeys the empirical relation [6] $E_d = \beta N_c Z_a N_e$, where N_c stands for the effective As coordination number, Z_a is the formal chemical valency of the chalcogen atom, N_e is the number of valence electrons per chalcogen atom and, in the particular case of our alloys, which are basically covalent, the constant β takes the value $0.37 \pm 0.04\,eV$ [6]. Since the chemical compositions of our samples, $As_{40}S_{60}$ and $As_{40}Se_{60}$, have a similar stoichiometry, the parameters Z_a and N_e take in both cases the values 2 and 28/3, respectively, and the effective As coordination number, N_c, can be therefore estimated from the values of E_d (see Table 1). The higher N_c values in the case of the $As_{40}Se_{60}$ films, either deposited by PECVD or TE, compared to the $As_{40}S_{60}$ films, suggest a higher interaction between the structural layers in the former. Such an interaction would be established through As atoms acting as bonding points forming $As \cdots Se$ intermolecular bonds, which would contribute to increase the effective As coordination number.

Infrared transmission spectra of amorphous PECVD As–S films have shown the presence of molecular species such as As_4S_4 (absorption bands at 346 and $374\,cm^{-1}$) and As_4S_3 (341 and $370\,cm^{-1}$) [17]. However, As–Se alloys are more reluctant to form such molecular units containing homopolar bonds compared to As–S alloys, and the virtual absence of As_4Se_4 molecules in the case of PECVD As–Se alloys has been confirmed by means of Raman spectroscopy [17]. Therefore, these molecular clusters would make difficult the cohesion between the structural layers in the case of the amorphous $As_{40}S_{60}$ films, and, consequently, would also contribute to decrease N_c. Nevertheless, on the basis of the values of E_d found, it seems reasonable to infer that the concentration of the above-introduced molecular clusters in the PECVD $As_{40}S_{60}$ films, is lower than in the TE ones, having the same composition. On the contrary, the almost complete absence of these molecular units in the As–Se alloys deposited by both techniques, along with the above-mentioned higher interaction of structural layers, would contribute to increase N_c as found by us. The influence of the deposition technique on the structural and optical properties of the $As_{40}Se_{60}$ films seems to be, therefore, not very significant.

The X-ray diffraction patterns displayed in Fig. 3 show significant structural differences between the PECVD films and the TE ones. In both alloys the FSDP for the PECVD films has a lower intensity, and is somewhat broader and shifted to the right ($\Delta(2\theta) = +0.98°$, for the a-$As_{40}S_{60}$ alloy, and $\Delta(2\theta) = +0.90°$, for a-$As_{40}Se_{60}$). Furthermore, in the case of the a-$As_{40}S_{60}$ film, the second diffuse peak changes notably. These results suggest, according to Elliott's model, that the PECVD technique would favor the compactness of the deposited films, in comparison with the TE. Nevertheless, the influence of the deposition technique seems to be more important for the S-based alloys compared to the Se-based ones. This is in agreement with the higher values of E_d found and, in turn, the higher values of N_c inferred, for the PECVD $As_{40}S_{60}$ films, in comparison with the TE ones. In addition, this also would explain why the values for these two parameters are quite similar in the case of the Se-based alloys, prepared by both techniques. From our X-ray diffraction results, it seems reasonable to assume that the concentration of As_4S_4 and/or As_4S_3 clusters must be lower in those samples deposited by PECVD. On the other hand, the structural disorder in the case of the a-As_2Se_3 films seems to be similar, irrespective of the preparation technique employed.

The optical-absorption spectra, $\alpha(\hbar\omega)$, derived by using the expressions corresponding to the envelope method for films with non-uniform thickness [3], are displayed in Fig. 4. The typical dependence of $\log \alpha(\hbar\omega)$ for an amorphous solid, with a clear absorption edge, is observed. The differences between the values of the absorption coefficient for the a-$As_{40}Se_{60}$ alloys prepared by PECVD and TE are less significant than those found in the case of the a-$As_{40}S_{60}$ films. This observation points out the slight influence that the deposition

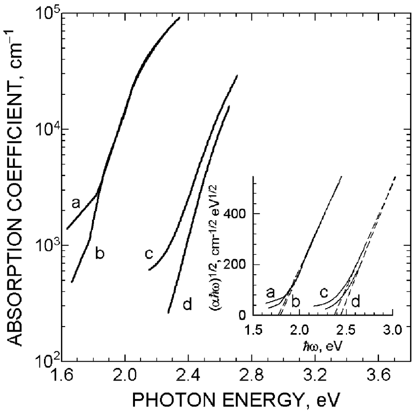

Fig. 4. Optical absorption spectra for PECVD $As_{40}Se_{60}$ (a), TE $As_{40}Se_{60}$ (b), PECVD $As_{40}S_{60}$ (c) and TE $As_{40}S_{60}$ (d) films. The corresponding so-called Tauc plots for the calculation of E_g^{opt} and $B^{1/2}$ are shown in the inset.

technique has on the optical properties of $As_{40}Se_{60}$ films, as indicated above.

The optical band gap, E_g^{opt}, is formally defined from the non-direct transition model proposed by Tauc [18], $(\alpha\hbar\omega)^{1/2} = B^{1/2}\ (\hbar\omega - E_g^{opt})$, as the intersection with the energy axis of the straight line through the high-energy points of a graph of $(\alpha\hbar\omega)^{1/2}$ versus $\hbar\omega$ (see the inset in Fig. 4). The parameter $B^{1/2}$ is the Tauc slope, which has been shown [19] to be inversely related to the degree of structural randomness in amorphous materials. Values for E_g^{opt} and $B^{1/2}$ determined from the absorption data shown in Fig. 4, are listed in Table 1. As expected in the light of the E_o values, the values of the Tauc gap are also higher in the case of the $As_{40}S_{60}$ films than in As–Se alloys, which can be explained considering the higher bonding energy of the As–S bond (379.5 kJ/mol), in comparison with the As–Se bond (96 kJ/mol). The difference between the E_g^{opt} values is larger for the As–S alloys prepared by PECVD and TE, than for the As–Se ones, which is very small. This result would support the fact that $As_{40}S_{60}$ films deposited by PECVD have lower concentration of molecular clusters containing homopolar bonds, compared with those prepared by TE, in contrast to the As–Se system. As already introduced, the bonding energies for As–As and S–S bonds are 382.0 and 425.3 kJ/mol, respectively, and thus, their higher or lower concentration in the material would affect the value of E_g^{opt} in the same way.

Finally, the values obtained for $B^{1/2}$ reflect that the films deposited by TE have a more ordered structure compared with those prepared by PECVD, which is in agreement with the X-ray diffraction data. As we mentioned before, the TE $As_{40}S_{60}$ film shows a FSDP whose intensity is higher than that corresponding to the PECVD film. Although in the case of $As_{40}Se_{60}$ films the values of $B^{1/2}$ are very close, they are still lower for the PECVD films.

5. Conclusions

Amorphous $As_{40}S_{60}$ and $As_{40}Se_{60}$ films have been prepared by PECVD and TE. The influence of the deposition technique is more significant in the case of the S-based alloys as compared with those of selenium alloys. Furthermore, the films prepared by PECVD seem to present a more compact structure, compared with those deposited by TE. Nevertheless, X-ray diffraction results suggest that the TE films have a more ordered structure, possibly due to the presence of As_4S_4 molecular units. Finally, the differences found between the values of the Tauc gaps and slopes support the structural conclusions derived in this work by means of other techniques.

References

[1] S.R. Elliott, Physics of Amorphous Materials, 2nd Ed., Longman, London, 1990.
[2] R. Glang, in: L.I. Maissel, R. Glang (Eds.), Handbook of Thin Film Technology, McGraw-Hill, New York, 1983.
[3] J.M. González-Leal, R. Prieto-Alcón, J.A. Angel, D.A. Minkov, E. Márquez, Appl. Optics 41 (2002) 34.
[4] R. Swanepoel, J. Phys. E.: Sci. Instrum. 17 (1984) 896.
[5] R. Swanepoel, S. Afr. J. Phys. 12 (1989) 148.
[6] S.H. Wemple, Phys. Rev. B 7 (1973) 3767.
[7] S.R. Elliott, Nature 354 (1991) 445.
[8] J.B. Ramírez-Malo, E. Márquez, C. Corrales, P. Villares, R. Jiménez-Garay, Mater. Sci. Eng. B. 25 (1994) 53.
[9] F.W. Glaze, D.H. Blackburn, J.S. Osmalov, D. Hubbard, M.H. Black, J. Res. Nat. Bur. Stand. 59 (1957) 2774.
[10] W.S. Rodney, I.J. Malitson, T.A. King, J. Opt. Soc. Am. 48 (1958) 633.
[11] R.K. Galkiewicz, J. Tauc, Solid State Commun. 10 (1972) 1261.
[12] Ke. Tanaka, Thin Solid Films 66 (1980) 271.
[13] E. Márquez, J.B. Ramírez-Malo, P. Villares, R. Jiménez-Garay, R. Swanepoel, Thin Solid Films 254 (1995) 83.
[14] K. Petkov, P.J.S. Ewen, J. Non-Cryst. Solids 249 (1999) 150.
[15] C. Corrales, Tesis Doctoral, Universidad de Cádiz, 1994.
[16] J.M. González-Leal, R. Prieto-Alcón, J.A. Angel, E. Márquez, J. Non-Cryst. Solids 315 (2003) 134.
[17] P. Nagels, Semiconductors 32 (1998) 32.
[18] J. Tauc, in: J. Tauc (Ed.), Amorphous and Liquid Semiconductors, Plenum, New York, 1974.
[19] A.R. Zanatta, I. Chambouleyron, Phys. Rev. B 53 (1996) 3833.